Riemannian Formulation and Comparison of Color Difference Formulas

Dibakar Raj Pant[1,2] and Ivar Farup[1]

[1]The Norwegian Color Research Laboratory,
Gjøvik University College, Norway
[2]The Laboratoire Hubert Curien,
University Jean Monnet, Saint Etienne, France

Abstract

Study of various color difference formulas by the Riemannian approach is useful. By this approach, it is possible to evaluate the performance of various color difference fourmlas having different color spaces for measuring visual color difference. In this paper, the authors present mathematical formulations of CIELAB (ΔE^*_{ab}), CIELUV (ΔE^*_{uv}), OSA-UCS (ΔE_E) and infinitesimal approximation of CIEDE2000 (ΔE_{00}) as Riemannian metric tensors in a color space. It is shown how such metrics are transformed in other color spaces by means of Jacobian matrices. The coefficients of such metrics give equi-distance ellipsoids in three dimensions and ellipses in two dimensions. A method is also proposed for comparing the similarity between a pair of ellipses. The technique works by calculating the ratio of the area of intersection and the area of union of a pair of ellipses. The performance of these four color difference formulas is evaluated by comparing computed ellipses with experimentally observed ellipses in the xy chromaticity diagram. The result shows that there is no significant difference between the Riemannized ΔE_{00} and the ΔE_E at small colour difference, but they are both notably better than ΔE^*_{ab} and ΔE^*_{uv}.

Introduction

Color difference metrics are in general derived from two kinds of experimental data. The first kind is threshold data obtained from color matching experiments and they are described by just noticeable difference (JND) ellipses. The second kind is visual colour difference data and it gives supra-threshold colour difference ellipses [1]. For example, Friele-MacAdam-Chickering (FMC) colour difference metric [2] is based on first kind of data where as the CIELAB [3] is based on second kind data.

MacAdam [4] was the first to describe just noticeable difference (JND) ellipses. Later, more elaborated data sets were established by Brown [5], Wyszecki and Fielder [6]. Examples of supra-threshold colour difference based data are BFD-Perceptibility(BFD-P) [7], RIT-DuPont [8], Witt [9]and others. The former two data sets were also included in the BFD-P data sets and fitted in the CIE xy chromaticity diagram [7].

Riemann [10] was the first to propose that colors, as well as the other objects of sense, could be described by non-Euclidean geometry. Later, Helmholtz [11] derived the first line element for a color space. Similarly, Schrödinger [12] and Stiles [13] also elaborated more on Helmholtz's line element with modifications. The latest and most advanced contribution along this line, is the zone-fluctuation line element of Vos and Walraven [14]. A thorough review of color metrics following the line element can be found in [15–17].

On the other side, color and imaging industries have a continuous demand for a practical standard for measuring perceptual color differences accurately. So, at present, many color difference metrics are in existence. Among these, the CIELAB and the CIELUV [3] are popular and the most established ones in industries. Theses formulas are defined by Euclidean metrics in their own color spaces that are obtained by non-linear transformations of the tristimulus values. The CIEDE2000 [18] is a revised and improved formula based on the CIELAB color space, resulting in a non-Euclidean metric. Another important example is the recent Euclidean color difference metric, ΔE_E proposed by Oleari [19] based on the OSA-UCS color space. However, all the formulas mentioned above have some demerits to measure the visual perception of the color differences sufficiently [20–24]. Further, it has also been noticed by many other color researchers that the small color difference calculation using the Euclidean distance does not agree sufficiently with the perceptual color difference due to the curvilinear nature of the color space [22, 25–29].

Studying the various color difference metrics by treating the color spaces as Riemannian spaces proves useful. In such a representation, one can map or transfer a color metric between many color spaces. Basically, in a curved space the shortest length or the distance between any two points is called a geodesic. In the Riemannian geometry, distances are defined in the similar way. Therefore, small color differences can be represented by an infinitesimal distance at a given point in a color space. This distance is given by a positive definite quadratic differential form, also known as the Riemannian metric. In this sense, the Riemannian metric provides a powerful mathematical tool to formulate metric tensors of different color difference formulas.These metric tensors allow us to compute equi-distance ellipses which can be analyzed and compared with experimentally observed ellipses in a common color space.

In this paper, the authors formulate the CIELAB, the CIELUV, and the OSA-UCS based ΔE_E color difference formulas in terms of Riemannian metric. Similarly, Riemannian approximation of the CIEDE2000 is also presented. The CIEDE2000 approximation is hereafter referred to as the Riemannized ΔE_{00}. This is done by taking the line element to calculate infinitesimal color differences dE. In this process, color difference equations are converted into the differential form. Again, to obtain the Riemannian metric in a new color space, we need to transform color vectors from one color space to another. This is accomplished by the Jacobian transformation. To illustrate the method, the authors transformed the four color difference formulas mentioned above into the xyY color space. The equi-distance ellipses of each formula are plotted in the xy chromaticity diagram for constant luminance. The input data to compute the ellipses for our method is the BFD-P data sets [7]. The BFD-P data sets were assessed by about 20 observers using a ratio method, and the chromaticity discrimination ellipses were calculated and plotted in the xy chromaticity diagram for each set [30]. A comparison has also been done between the computed equi-distance ellipses of each formula and the original ellipses obtained from the BFD-P data set. A method for comparing a pair of ellipses by calculating the ratio of the area of intersection and the area of union was proposed by the authors [31]. This method gives a single comparison value which takes account of variations in the size, the shape and the orientation simultaneously for a pair of ellipses. Therefore, this value is an indicator which tells us how well two ellipses match each other. A comparative analysis has also discussed between computed equi-distance ellipses of different color difference formulas.

Method

Ellipse Equation

In the Riemannian space, a positive definite symmetric metric tensor g_{ik} is a function which is used to compute the infinitesimal distance between any two points. So, the arc length of a curve between two points is expressed by a differential quadratic form as given below :

$$ds^2 = g_{11}dx^2 + 2g_{12}dxdy + g_{22}dy^2. \tag{1}$$

The matrix form of Equation (1) is

$$ds^2 = \begin{bmatrix} dx & dy \end{bmatrix} \begin{bmatrix} g_{11} & g_{12} \\ g_{12} & g_{22} \end{bmatrix} \begin{bmatrix} dx \\ dy \end{bmatrix}, \tag{2}$$

and

$$g_{ik} = \begin{bmatrix} g_{11} & g_{12} \\ g_{21} & g_{22} \end{bmatrix} \tag{3}$$

where ds is the distance between two points, dx is the difference of x coordinates, dy is the difference of y coordinates and g_{11}, g_{12} and g_{22} are the coefficients of the metric tensor g_{ik}. Here, the coefficient g_{12} is equal to the coefficient g_{21} due to symmetry.

In a two dimensional color space, the metric g_{ik} gives the intrinsic properties about the color measured at a surface point. Specifically, the metric represents the chromaticity difference of any two colors measured along the geodesic of the surface.In general, it gives equi-distant contours. However, to calculate small colour differences considering infinitesimal distance ds, the coefficients of g_{ik} also determine an ellipse in terms of its parameters and vice versa. The parameters are the semimajor axis, a, the semiminor axis, b, and the angle of inclination in a geometric plane, θ, respectively. In equation form, the coefficients of g_{ik} in terms of the ellipse parameter are expressed as [31]:

$$\begin{aligned} g_{11} &= \frac{1}{a^2}\cos^2\theta + \frac{1}{b^2}\sin^2\theta, \\ g_{12} &= \cos\theta\sin\theta\,(\frac{1}{a^2} - \frac{1}{b^2}), \\ g_{22} &= \frac{1}{a^2}\sin^2\theta + \frac{1}{b^2}\cos^2\theta. \end{aligned} \tag{4}$$

The angle formed by the major axis with the positive x-axis is given by

$$\tan(2\theta) = \frac{2g_{12}}{(g_{11} - g_{22})}. \tag{5}$$

Here $\theta \leq 90^\circ$ when $g_{12} \leq 0$, and otherwise $\theta \geq 90^\circ$. Similarly, the inverse of Equations (4–5) are

$$\begin{aligned} \frac{1}{a^2} &= g_{22} + g_{12}\cot\theta, \\ \frac{1}{b^2} &= g_{11} - g_{12}\cot\theta. \end{aligned} \tag{6}$$

Alternatively, the semi major axis, a, and the semi minor axis, b, of an ellipse can also be determined by the eigenvector and eigenvalue of the metric g_{ik}. If λ_1 and λ_2 are eigenvalues of the metric g_{ik}, the semimajor axis, a, and the semiminor axis, b, equal to $1/\sqrt{\lambda_1}$ and $1/\sqrt{\lambda_2}$ respectively. Like wise, θ is the angle between the first eigenvector and the first axis [32].

Transformation of coordinates

In Equation (1), the quantity ds^2 is called the first fundamental form which gives the metric properties of a surface. Now, suppose that x and y are related to another pair of coordinates u and v. Then, these new coordinates will also have new metric tensor g'_{ik}. As analogy to Equation (3), it is written as:

$$g'_{ik} = \begin{bmatrix} g'_{11} & g'_{12} \\ g'_{21} & g'_{22} \end{bmatrix}. \tag{7}$$

Now, the new metric tensor g'_{ik} is related to g_{ik} via the matrix equation as follows:

$$\begin{bmatrix} g'_{11} & g'_{12} \\ g'_{21} & g'_{22} \end{bmatrix} = \begin{bmatrix} \frac{\partial x}{\partial u} & \frac{\partial x}{\partial v} \\ \frac{\partial y}{\partial u} & \frac{\partial y}{\partial v} \end{bmatrix}^T \begin{bmatrix} g_{11} & g_{12} \\ g_{21} & g_{22} \end{bmatrix} \begin{bmatrix} \frac{\partial x}{\partial u} & \frac{\partial x}{\partial v} \\ \frac{\partial y}{\partial u} & \frac{\partial y}{\partial v} \end{bmatrix}, \tag{8}$$

where the superscript T denotes the matrix transpose and the matrix

$$J = \frac{\partial(x, y)}{\partial(u, v)} = \begin{bmatrix} \frac{\partial x}{\partial u} & \frac{\partial x}{\partial v} \\ \frac{\partial y}{\partial u} & \frac{\partial y}{\partial v} \end{bmatrix} \tag{9}$$

is the Jacobian matrix for the coordinate transformation, or, simply, the Jacobian.

Ellipse comparison

Using the principles of union–intersection and ratio testing, the authors present the method to compare two ellipses with respect to their size, shape and orientation. Figure 1(a) shows two ellipses A and B. The common area is the intersection area between them and the total area of A and B is known as the union area. From the statistical point of view, the acceptance region is the intersection area and the rejection region is the union area. The ratio of these intersection and union area gives us a non-negative value which lies in the range of $0 < x \leq 1$. So, the matching ratio is expressed as:

$$R = \frac{\text{Area}(\text{A} \bigcap B)}{\text{Area}(A \bigcup B)} \tag{10}$$

High value of R gives strong evidence that the two ellipses are closely matched and vice versa. For example, a highly matched ellipse pair with R equal to .92 and a poorly matched ellipse pair with R equal to .21 are shown in Figure 1(b) and Figure 1(c) respectively. Hence, a match ratio of 1 between a pair of ellipses ensures full matching between them in terms of size, shape and orientation.

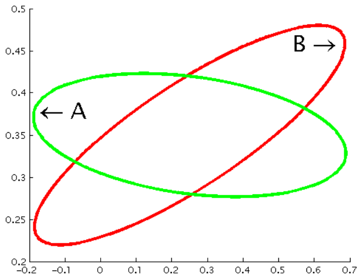

(a) The union and the intersection area of two ellipses.

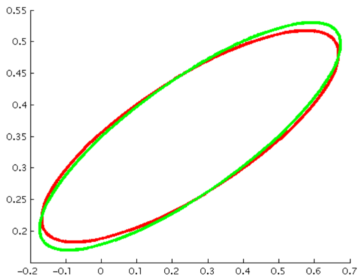

(b) Highly matched ellipse pair with R .92.

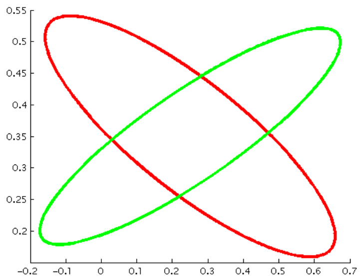

(c) Poorly matched ellipse pair with R .21.

Figure 1: Illustration of the method to compare two ellipses with respect to their size, shape and orientation.

The Color Difference Metrics

In this section, the authors show how to derive the Riemannian forms of the four color difference metrics chosen for the study. Only the outline of the derivations are given. For the detailed expressions of the coefficients of the Jacobian matrices, see the appendix.

The ΔE^*_{ab} Metric

The color difference in the CIELAB color space is defined as the Euclidean distance,

$$\Delta E^*_{ab} = \sqrt{(\Delta L^*)^2 + (\Delta a^*)^2 + (\Delta b^*)^2}\,. \tag{11}$$

The CIELAB color space defined for moderate to high lightness is given as

$$\begin{aligned} L^* &= 116\left(\frac{Y}{Y_r}\right)^{\frac{1}{3}} - 16, \\ a^* &= 500\left[\left(\frac{X}{X_r}\right)^{\frac{1}{3}} - \left(\frac{Y}{Y_r}\right)^{\frac{1}{3}}\right], \\ b^* &= 200\left[\left(\frac{Y}{Y_r}\right)^{\frac{1}{3}} - \left(\frac{Z}{Z_r}\right)^{\frac{1}{3}}\right], \end{aligned} \tag{12}$$

where L^*, a^* and b^* corresponds to the Lightness, the redness-greenness and the yellowness-blueness scales in the CIELAB color space. Similarly, X, Y, Z and X_r, Y_r, Z_r are the tristimulus values of the color stimuli and white reference respectively.

The relationship between X, Y and Z tristimulus coordinates and x, y and Y color coordinates are

$$\begin{aligned} X &= \frac{xY}{y}, \\ Y &= Y, \\ Z &= \frac{(1-x-y)Y}{y}\,. \end{aligned} \tag{13}$$

If we take the line element distance to measure the infinitesimal color difference at a point in the color space, Equation (11) becomes differential. In terms of the differential quadratic form, we can write

$$(dE^*_{ab})^2 = \begin{bmatrix} dL^* & da^* & db^* \end{bmatrix} \begin{bmatrix} dL^* \\ da^* \\ db^* \end{bmatrix}. \tag{14}$$

Now, to transfer or map differential color vectors dL^*, da^*, db^* into dX, dY, dZ tristimulus color space, it is necessary to apply the Jacobian transformation where the variables of two color spaces are related by continuous partial derivatives. Hence, it is expressed as:

$$\begin{bmatrix} dL^* \\ da^* \\ db^* \end{bmatrix} = \begin{bmatrix} \frac{\partial L}{\partial X} & \frac{\partial L}{\partial Y} & \frac{\partial L}{\partial Z} \\ \frac{\partial a}{\partial X} & \frac{\partial a}{\partial Y} & \frac{\partial a}{\partial Z} \\ \frac{\partial b}{\partial X} & \frac{\partial b}{\partial Y} & \frac{\partial b}{\partial Z} \end{bmatrix} \begin{bmatrix} dX \\ dY \\ dZ \end{bmatrix}. \tag{15}$$

Again, from Equations (14) and (15), we have

$$(dE^*_{ab})^2 = \begin{bmatrix} dX dY dZ \end{bmatrix} \frac{\partial(L, a^*, b^*)}{\partial(X, Y, Z)}^T \frac{\partial(L, a^*, b^*)}{\partial(X, Y, Z)} \begin{bmatrix} dX \\ dY \\ dZ \end{bmatrix}, \tag{16}$$

where $\partial(L, a^*, b^*)/\partial(X, Y, Z)$ is the Jacobian matrix in Equation (15).

Similarly, transformation from X, Y, Z tristimulus color space into x, y, Y color space is done by another Jacobian matrix $\partial(X, Y, Z)/\partial(x, y, Y)$ and expressed as :

$$\begin{bmatrix} dX \\ dY \\ dZ \end{bmatrix} = \begin{bmatrix} \frac{\partial X}{\partial x} & \frac{\partial X}{\partial y} & \frac{\partial X}{\partial Y} \\ \frac{\partial Y}{\partial x} & \frac{\partial Y}{\partial y} & \frac{\partial Y}{\partial Y} \\ \frac{\partial Z}{\partial x} & \frac{\partial Z}{\partial y} & \frac{\partial Z}{\partial Y} \end{bmatrix} \begin{bmatrix} dx \\ dy \\ dY \end{bmatrix}. \tag{17}$$

Finally, the L^*, a^*, b^* metric is transformed into x, y, Y as follows:

$$(dE^*_{ab})^2 = \begin{bmatrix} dx & dy & dY \end{bmatrix} \frac{\partial(X, Y, Z)}{\partial(x, y, Y)}^T \frac{\partial(L, a^*, b^*)}{\partial(X, Y, Z)}^T \frac{\partial(L, a^*, b^*)}{\partial(X, Y, Z)} \frac{\partial(X, Y, Z)}{\partial(x, y, Y)} \begin{bmatrix} dx \\ dy \\ dY \end{bmatrix}. \tag{18}$$

Thus, the Riemannian metric tensor corresponding to ΔE^*_{ab} in the xyY space is

$$g_{\Delta E^*_{ab}} = \frac{\partial(X, Y, Z)}{\partial(x, y, Y)}^T \frac{\partial(L, a^*, b^*)}{\partial(X, Y, Z)}^T \frac{\partial(L, a^*, b^*)}{\partial(X, Y, Z)} \frac{\partial(X, Y, Z)}{\partial(x, y, Y)}. \tag{19}$$

The ΔE^*_{uv} Metric

The color difference in the CIELUV color space is defined as the Euclidean distance,

$$\Delta E^*_{uv} = \sqrt{(\Delta L^*)^2 + (\Delta u^*)^2 + (\Delta v^*)^2}. \tag{20}$$

The CIELUV color space is defined as

$$\begin{aligned} L^* &= 116 \left(\frac{Y}{Y_r}\right)^{\frac{1}{3}} - 16, \\ u^* &= 13L \left[\left(\frac{4X}{X + 15Y + 3Z}\right) - \left(\frac{4X_r}{X_r + 15Y_r + 3Z_r}\right)\right], \\ v^* &= 13L \left[\left(\frac{9Y}{X + 15Y + 3Z}\right) - \left(\frac{9Y_r}{X_r + 15Y_r + 3Z_r}\right)\right]. \end{aligned} \tag{21}$$

In complete analogy with the case for ΔE^*_{ab}, the Riemannian metric tensor corresponding to ΔE^*_{uv} in the xyY space is

$$g_{\Delta E^*_{uv}} = \frac{\partial(X, Y, Z)}{\partial(x, y, Y)}^T \frac{\partial(L, u^*, v^*)}{\partial(X, Y, Z)}^T \frac{\partial(L, u^*, v^*)}{\partial(X, Y, Z)} \frac{\partial(X, Y, Z)}{\partial(x, y, Y)}. \tag{22}$$

The Riemannized ΔE_{00} Metric

The CIEDE2000 formula derived from the CIELAB color space is defined as a non-Euclidean metric in a space as follows :

$$\Delta E_{00} = \left[\left(\frac{\Delta L'}{k_L S_L} \right)^2 + \left(\frac{\Delta C'}{k_C S_C} \right)^2 + \left(\frac{\Delta H'}{k_H S_H} \right)^2 + R_T \left(\frac{\Delta C'}{k_C S_C} \right) \left(\frac{\Delta H'}{k_H S_H} \right) \right]^{0.5}. \tag{23}$$

The rotation function, R_T, is defined as:

$$R_T = -\sin(2\Delta\theta) R_c, \tag{24}$$

$$\text{where } \Delta\theta = 30 \cdot \exp\left[-\left(\frac{\bar{h}' - 275}{25} \right)^2 \right], \tag{25}$$

$$\text{and } R_c = 2\sqrt{\frac{\bar{C'}^7}{\bar{C'}^7 + 25^7}}\,. \tag{26}$$

The weighting functions are defined as:

$$S_L = 1 + \frac{0.015(\bar{L}' - 50)^2}{\sqrt{20 + (\bar{L}' - 50)^2}}, \tag{27}$$

$$S_C = 1 + 0.045\bar{C}', \tag{28}$$

$$S_H = 1 + 0.015\bar{C}'T, \tag{29}$$

$$\text{with } T = 1 - 0.17\cos(\bar{h}' - 30^o) + 0.24\cos(2\bar{h}') + .32\cos(3\bar{h}' + 6^o) - 0.2\cos(4\bar{h}' - 63^o). \tag{30}$$

Here, the lightness, the chroma and the hue are obtained taking the average of the pair of color samples for which the color difference is to be determined, $\bar{L}' = (L_1' + L_2')/2$, $\bar{C}' = (C_1' + C_2')/2$ and $\bar{h}' = (h_1' + h_2')/2$. Further, $\Delta H' = 2\sqrt{C_1' C_2'}\sin(\Delta h'/2)$.

The color coordinates used in the formula are defined from the CIELAB coordinates in the following way:

$$L' = L^*, \tag{31}$$

$$a' = a^*(1 + G), \tag{32}$$

$$b' = b^*, \tag{33}$$

$$C' = \sqrt{a'^2 + b'^2}\,, \tag{34}$$

$$h' = \arctan\frac{b'}{a'}\,, \tag{35}$$

$$G = \frac{1}{2}\left(1 - \sqrt{\frac{C_{ab}^{*7}}{C_{ab}^{*7} + 25^7}} \right), \tag{36}$$

where L^*, a^* and b^* corresponds to the lightness, the redness-greenness and the yellowness-blueness scales and C^* chroma in the CIELAB color space. Likewise, h' is the hue angle for a pair of samples. The authors like to explain some problems for formulating Riemannian metric of ΔE_{00}. In the ΔE_{00} formula as given in Equation (23), the coordinate H' does not exist since $\Delta H'$ is not the difference of any H'. As per the rules of Riemannian geometry, it is not possible to get the Riemannian metric of the formula from its original configuration. However, at infinitesimal colour difference, it is possible to use $L'C'h'$ coordinates instead of $L'C'H'$ because $C^{'}$ and $h^{'}$ are legitimate coordinates. Calculation of Riemannian metric using $L'C'h'$ coordinates gives us an approximation of ΔE_{00} when we substitute $dH' = C'dh'$ as proposed by Völz [33] at infinitesimal colour difference only. But, this Riemannized ΔE_{00} can not be integrated to build CIE defined ΔE_{00} due to the definition of $\Delta H'$. Defining the metric for infinitesimal colour differences, the discontinuity problems in the hue angle as noted by Sharma et.al. [34] vanish. This is due to taking h' values instead of taking airthmetic mean $\bar{h}'$. However, there are very small discontinuities remaining in R_T, caused by the discontinuity of h' at $h' = 0$ and in the transformation from XYZ to $L^*a^*b^*$.

To calculate line element L', C' and h' values are taken. So, the Equation (23) in the approximate differential form is written as follows:

$$\begin{aligned}(dE_{00})^2 &= \begin{bmatrix} dL' & dC' & dh' \end{bmatrix} \\ &\times \begin{bmatrix} (k_L S_L)^{-2} & 0 & 0 \\ 0 & (k_C S_C)^{-2} & \frac{1}{2} C^{'} R_T (k_C S_C k_H S_H)^{-1} \\ 0 & \frac{1}{2} C^{'} R_T (k_C S_C k_H S_H)^{-1} & C^{'2} (k_H S_H)^{-2} \end{bmatrix} \\ &\times \begin{bmatrix} dL' \\ dC' \\ dh' \end{bmatrix}. \end{aligned} \tag{37}$$

In Equation (37), the matrix consisting of weighting functions, parametric factors, and rotation term is the Riemannian metric of the formula in its approximate form. This metric is positive definite since $R_T^2/4 < 1$, $\sin(2\Delta\theta) \in [-1, 1]$ and $|R_C| < 2$ (see Equations (24)–(26)). It can be transformed into xyY color space by the Jacobian method. The first step is to transform differential color vectors $[dL'\, dC'\, dh']$ into $[dL^{'}\, da^{'}\, db^{'}]$ by computing all partial derivatives of vector functions L', C', and h' with respect to $L^{'}$, $a^{'}$, and $b^{'}$. Then, the $L^{'}$, $a^{'}$, and $b^{'}$ differential vecors are again transformed into L^*, a^*, and b^* . Rest of the other process is analog to the CIELAB space. The resulting Riemannian metric tensor representing the CIEDE2000 color difference metric in the xyY space is

$$\begin{aligned} g_{\Delta E_{00}} = &\frac{\partial(X,Y,Z)}{\partial(x,y,Y)}^T \frac{\partial(L,a^*,b^*)}{\partial(X,Y,Z)}^T \frac{\partial(L',a',b')}{\partial(L,a^*,b^*)}^T \frac{\partial(L',C',h')}{\partial(L^{'},a^{'},b^{'})}^T \\ &\times \begin{bmatrix} (k_L S_L)^{-2} & 0 & 0 \\ 0 & (k_C S_C)^{-2} & \frac{1}{2} C^{'} R_T (k_C S_C k_H S_H)^{-1} \\ 0 & \frac{1}{2} C^{'} R_T (k_C S_C k_H S_H)^{-1} & C^{'2} (k_H S_H)^{-2} \end{bmatrix} \\ &\times \frac{\partial(L',C',h')}{\partial(L^{'},a^{'},b^{'})} \frac{\partial(L',a',b')}{\partial(L,a^*,b^*)} \frac{\partial(L,a^*,b^*)}{\partial(X,Y,Z)} \frac{\partial(X,Y,Z)}{\partial(x,y,Y)}. \end{aligned} \tag{38}$$

The ΔE_E Metric

The ΔE_E color difference formula is defined as the Euclidean metric in the log compressed OSA-UCS color space,

$$\Delta E_E = \sqrt{(\Delta L_E)^2 + (\Delta G_E)^2 + (\Delta J_E)^2} \, . \tag{39}$$

Here, L_E G_E and J_E are the coordinates in the log-compressed OSA-UCS space. The lightness is derived from the original OSA-UCS formula and their definitions are expressed as follows[35, 36]:

$$\begin{aligned}
L_E &= \left(\frac{1}{b_L}\right) \ln\left[1 + \frac{b_L}{a_L}(10L_{OSA})\right], && (40)\\
C_E &= \left(\frac{1}{b_c}\right) \ln\left[1 + \frac{b_c}{a_c}(10C_{OSA})\right], && (41)\\
C_{OSA} &= \sqrt{G^2 + J^2}, && (42)\\
h &= \arctan(\frac{-J}{G}), && (43)\\
G_E &= -C_E \cos(h), && (44)\\
J_E &= C_E \sin(h), && (45)
\end{aligned}$$

with the following constants,

$$\begin{aligned}
a_L &= 2.890,\\
b_L &= 0.015,\\
a_c &= 1.256,\\
b_c &= 0.050.
\end{aligned} \tag{46}$$

Expressing G_E and J_E in terms of C_{OSA}, we have:

$$\begin{aligned}
\cos h &= \frac{G}{\sqrt{G^2 + J^2}} \, ,\\
\sin h &= \frac{-J}{\sqrt{G^2 + J^2}} \, ,\\
G_E &= -\frac{C_E G}{C_{OSA}} \, ,\\
J_E &= -\frac{C_E J}{C_{OSA}} \, .
\end{aligned} \tag{47}$$

The OSA-UCS color space is in turn related to the CIEXYZ color space:

$$\begin{aligned}
L_{OSA} &= \left(5.9[(Y_0^{1/3} - \frac{2}{3}) + 0.042(Y_0 - 30)^{1/3}] - 14.4\right) \frac{1}{\sqrt{2}},\\
Y_0 &= Y \left(4.4934x^2 + 4.3034y^2 - 4.2760xy - 1.3744x - 2.5643y + 1.8103\right) .
\end{aligned} \tag{48}$$

The coordinates J and G, which correspond to the empirical j and g of the OSA-UCS are defined through a sequence of linear transformations and a logarithmic compression as follows:

$$\begin{bmatrix} A \\ B \\ C \end{bmatrix} = \begin{bmatrix} 0.6597 & 0.4492 & -0.1089 \\ -0.3053 & 1.2126 & 0.0927 \\ -0.0374 & 0.4795 & 0.5579 \end{bmatrix} \begin{bmatrix} X \\ Y \\ Z \end{bmatrix}, \tag{49}$$

$$\begin{bmatrix} J \\ G \end{bmatrix} = \begin{bmatrix} S_J & 0 \\ 0 & S_G \end{bmatrix} \begin{bmatrix} -\sin\alpha & \cos\alpha \\ \sin\beta & -\cos\beta \end{bmatrix} \begin{bmatrix} \ln\left(\frac{A/B}{A_n/B_n}\right) \\ \ln\left(\frac{B/C}{B_n/C_n}\right) \end{bmatrix} \tag{50}$$

$$\begin{aligned} &= \begin{bmatrix} 2(0.5735L_{OSA} + 7.0892) & 0 \\ 0 & -2(0.764L_{OSA} + 9.2521) \end{bmatrix} \\ &\times \begin{bmatrix} 0.1792[\ln A - \ln(0.9366B)] + 0.9837[\ln B - \ln(0.9807C)] \\ 0.9482[\ln A - \ln(0.9366B)] - 0.3175[\ln B - \ln(0.9807C)] \end{bmatrix}. \end{aligned} \tag{51}$$

For calculating the line element at a given point, the log-compressed OSA-UCS formula given in Equation (39) is written as:

$$(dE_E)^2 = \begin{bmatrix} dL_E & dG_E & dJ_E \end{bmatrix} \begin{bmatrix} dL_E \\ dG_E \\ dJ_E \end{bmatrix}. \tag{52}$$

The differential color vectors can be transformed into the OSA-UCS color space by applying the Jacobian method as follows:

$$(dE_E)^2 = \begin{bmatrix} dL_{OSA} & dG & dJ \end{bmatrix} \frac{\partial(L_E, G_E, J_E)}{\partial(L_{OSA}, G, J)}^T \frac{\partial(L_E, G_E, J_E)}{\partial(L_{OSA}, G, J)} \begin{bmatrix} dL_{OSA} \\ dG \\ dJ \end{bmatrix}. \tag{53}$$

In the OSA-UCS space, the coordinates J and G are also related with the lightness function L_{OSA}. So, to transfer the differential color vectors $[dL_{OSA}\ dG\ dJ]$ into $[dx\,dy\,dY]$, it is required to split the differential lightness vector dL_{OSA} and the differential coordinates dG and dJ in two parts. At first, let us relate $[dL_{OSA}\,dG\,dJ]$ in terms of $[dx\,dy\,dY]$ as follows:

$$\begin{bmatrix} dL_{OSA} \\ dG \\ dJ \end{bmatrix} = \frac{\partial(L_{OSA}, G, J)}{\partial(x, y, Y)} \begin{bmatrix} dx \\ dy \\ dY \end{bmatrix} = \begin{bmatrix} \frac{\partial L_{OSA}}{\partial(x,y,Y)} \\ \frac{\partial(G,J)}{\partial(x,y,Y)} \end{bmatrix} \begin{bmatrix} dx \\ dy \\ dY \end{bmatrix}, \tag{54}$$

where $\partial(L_{OSA}, G, J)/\partial(x, y, Y)$ is a 3×3 Jacobian matrix that is further divided into the 1×3 and 2×3 Jacobian matrices $\partial L_{OSA}/\partial(x, y, Y)$ and $\partial(G, J)/\partial(x, y, Y)$, respectively. The first one is again separated as follows:

$$\frac{\partial L_{OSA}}{\partial(x, y, Y)} = \frac{\partial L_{OSA}}{\partial Y_0} \begin{bmatrix} \frac{\partial Y_0}{\partial x} & \frac{\partial Y_0}{\partial y} & \frac{\partial Y_0}{\partial Y} \end{bmatrix}. \tag{55}$$

Similarly, the second one is also separated in two parts since both G and J depends on x, y, Y not only through A, B, and C, but also through L_{OSA}. So, the Jacobian follows as:

$$\frac{\partial(G, J)}{\partial(x, y, Y)} = \frac{\partial(G, J)}{\partial(L_{OSA}, A, B, C)} \cdot \frac{\partial(L_{OSA}, A, B, C)}{\partial(x, y, Y)}. \tag{56}$$

Again, in Equation (56), the last Jacobian $\partial(L_{OSA}, A, B, C)/\partial(x, y, Y)$ is further split in two parts according to

$$\frac{\partial(L_{OSA}, A, B, C)}{\partial(x, y, Y)} = \begin{bmatrix} \frac{\partial L_{OSA}}{\partial(x,y,Y)} \\ \frac{\partial(A,B,C)}{\partial(x,y,Y)} \end{bmatrix}, \tag{57}$$

where

$$\frac{\partial(A, B, C)}{\partial(x, y, Y)} = \frac{\partial(A, B, C)}{\partial(X, Y, Z)} \frac{\partial(X, Y, Z)}{\partial(x, y, Y)}. \tag{58}$$

The first of these is simply the constant matrix given in Equation (49), and the last one is already familiar from the other metrics.

Results and Discussion

In this section, first, the authors discuss the behaviour of computed ellipses of the ΔE^*_{ab}, the ΔE^*_{uv}, the Riemannized ΔE_{00} and the ΔE_E in the xyY color space with respect to BFD-P ellipses individually. Secondly, a comparative study between computed ellipses of these four color difference metrics will be done.A detailed quantitative comparison is done by using BFD-P data sets.

Before doing comparative analysis, it is necessary to mention that equi-distance ellipses computed by the metric defined in Equation (38) represents Riemannized ΔE_{00} ellipses for infinitesimal colour differences. In fact, the ΔE_{00} metric in its original form does not define the Riemannian space in the strict sense.

Similarly, the ellipses are computed with a constant Y=0.4 in xyY color space. If we define constant lightness, then partial derivatives of lightness functions of all Jacobians will be zero. This gives 2×2 metric tensors and ellipses are computed in the xy chromaticity diagram.

Figure 2 shows BFD-P ellipses in the CIE 1964 chromaticity diagram. Similarly, Figures 3(a), 3(b), 3(c) and 3(d) show the ellipses of ΔE^*_{ab}, ΔE^*_{uv}, Riemannized ΔE_{00} and ΔE_E metrics respectively, using BFD-P data. All these ellipses are computed at the constant lightness value ($L^* = 50$) and color centers are taken from BFD-P data. In the xyY color space, this lightness value corresponds to the luminance $Y = 0.4$. In the Riemannized ΔE_{00} case, parametric factors (k_L, k_C and k_H) are set to 1. Comparing with BFD-P ellipses, disagreements can be seen with respect to the size, shape and rotation in ellipses of ΔE^*_{ab}, ΔE^*_{uv}, Riemannized ΔE_{00} and ΔE_E formulas. ΔE^*_{ab} and ΔE^*_{uv} ellipses appear more circular than BFD-P ellipses, but Riemannized ΔE_{00} and ΔE_E ellipses follow closer to the original ellipses in the blue and green region. However, it could be said that all computed ellipses of these four color difference metrics follow the general pattern of agreement with BFD-P ellipses. For example, the blue is the smallest, the green largest and the red, blue and yellow are more elongated than others. But, it is also seen that Riemannized ΔE_{00} and ΔE_E ellipses represent experimentally obtained ellipses more reasonably than compared to ΔE^*_{ab} and ΔE^*_{uv} ellipses. For example, ellipses of ΔE^*_{ab}, and ΔE^*_{uv} around neutral and gray color centers are bigger in size, while in the same region Riemannized ΔE_{00} and ΔE_E ellipses look more similar to the BFD-P ellipses. This indicates better quality performance of these two color difference formulas over two popular ΔE^*_{ab} and ΔE^*_{uv} formulas. Similarly, ΔE_E ellipses perform better in the blue region than Riemannized ΔE_{00} ellipses. The authors also computed the difference between the Riemannized ΔE_{00} and the original ΔE_{00} metrices for finite colour differences by using the CIEDE2000 total colour difference test data of Gaurav Sharma et.al. [34]. For $\Delta E_{00} \leq 1$, the error is less than 0.5% and for $\Delta E_{00} \leq 2$, it is smaller than 1.2%. However, It is seen that in the cases where $\Delta E_{00} > 2.5$, the error between two metrices steeply raise. But, for larger colour differences, geodesic line can be calculated from the metric tensor of the Riemannized ΔE_{00}. Basically, ΔE_{00} formula is developed to calculate small colour differences because the BFD-P data set upon which the ΔE_{00} formula developed is scaled for $\Delta E^*_{ab} < 2$ [7].

As described in the Ellipse Comparison part of the Methods section, the analysis is done by our method for comparing the similarity of a pair of ellipses. In Figure 4, histogram of R values between BFD-P and ΔE^*_{ab}, ΔE^*_{uv}, Riemannized ΔE_{00} and ΔE_E ellipses are given in Figures 4(a), 4(b), 4(c), 4(d) respectively. According to this method, the maximum R values given by ΔE^*_{ab}, ΔE^*_{uv}, Riemannized ΔE_{00} and ΔE_E are .81, .87, .95, and .93 respectively. Similarly, the lowest R values of these four formulas are, .1, .14, .2 and .2 respectively. Ellipse pairs of all metrics having maximum R values are located around neutral color region while matching pairs with lowest R are found around high chroma blue. Table 1 shows number of matching ellipses of four metrics with R values greater than .75 and less than .75. The result indicates that the Riemannized ΔE_{00} and ΔE_E perform better than the ΔE^*_{ab} and the ΔE^*_{uv}.

The authors have also used box plots to display ellipse matching values of these metrics in Figure 5. In the plots, the median value is marked by the central horizontal lines. The notch indicate the confidence interval of the median, and the box is bounded by the upper and lower quartiles of the grouped data. We can see that the Riemannized ΔE_{00} gives the highest median value while the CIELAB median value is the lowest. By using this technique, full range of matching value data is also plotted for comparing these four metrics simultaneously. The range of data is shown by dashed line, and outliers and marked with a cross. According to this box plot, the performance ranking of these metrics come in the following order: Riemannized ΔE_{00} first, ΔE_E second, ΔE^*_{uv} third and ΔE^*_{ab} fourth. However, there is no big difference between ΔE_{00} and ΔE_E and between ΔE^*_{uv} and ΔE^*_{ab}. But, with respect to Riemannized ΔE_{00} and ΔE_E, the performance of ΔE^*_{uv} and ΔE^*_{ab} metrics for matching ellipses is seen weaker.

In order to compare how well the different metrics reproduce the BFD-P ellipses, the pairwise statistical sign test of R values is also done between all pairs of metrics. The test result shows that at 5 % confidence level, Riemannized ΔE_{00} and ΔE_E both performed significantly better than ΔE^*_{uv} and ΔE^*_{ab} metrics. Further, ΔE^*_{uv} performs better than ΔE^*_{ab} with $p = 0.0176$. There is no significant difference between ΔE_{00} and ΔE_E metrics.

On the basis of above results, it is good to point the features of color spaces used by these metrics responsible for better performance. For example, saturation is defined in ΔE^*_{uv} not in ΔE^*_{ab} [37]. In ΔE_E, the lightness L_{OSA} takes into account the Helmholtz-Kohlrausch and crispening effects [19]. Further, the OSA-UCS system adopts a regular rhombohedral geometry which gives square grid with integer value of lightness [38]. This makes OSA-UCS space more uniform than CIELAB and CIELUV and suitable for small to medium color difference measurement. On the other hand, the non-Euclidean Riemannized

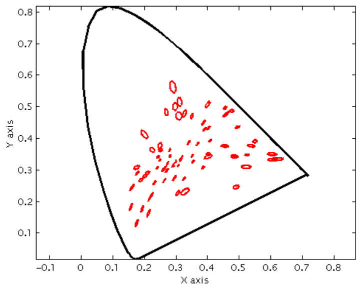

Figure 2: BFD-P ellipses in the CIE1964 chromaticity diagram (enlarged 1.5 times).

ΔE_{00} have many parameters for computing color differences. However, this formula has its specific advantage to correct the non-linearity of the visual system. But, the quality of the formula depends on selecting parameters values.

Table 1: Number of matching ellipses with matching values $\geq .75$ and $\leq .75$ of four color difference metrics. This matching is done with BFD-P ellipses.

	Number of Ellipse pairs with match ratio $\geq .75$	Number of Ellipse pairs with match ratio $\leq .75$
ΔE^*_{ab}	3	77
ΔE^*_{uv}	7	73
ΔE_{00}	57	23
ΔE_E	55	25

Conclusion

First, formulation of CIELAB, CIELUV, Riemannized CIEDE00 and OSA-UCS ΔE_E color difference formulas into the Riemannian metric is successfully accomplished. Secondly, The Riemannized ΔE_{00} is found indistinguishable to the exact ΔE_{00} for the small colour differences.

Thirdly, computation of equi-distance ellipses of these four formulas in the xyY color space is done by transferring Riemannian metrics of formulas into the xyY color space by the Jacobian method. Fourthly, a comparison between experimentally observed BFD-P and computed ellipses of these formulas is done in two ways: first descriptive and second by our developed comparison technique. On the basis of our findings as discussed above, the authors can say that Riemannized CIEDE2000 and OSA-UCS ΔE_E formulas measure the visual color differences significantly better than CIELAB and CIELUV formulas. However, neither formulas are fully perfect for matching visual color differences data. Among CIELAB and CIELUV formulas, performance of the CIELUV is found slightly better than the CIELAB. Similarly, there is no significant difference between Euclidean ΔE_E and Riemannized CIEDE2000 formulas. It is interesting to note that the Euclidean ΔE_E formula is not inferior to the complex, non-Euclidean industry standard ΔE_{00} for measuring small color differences.

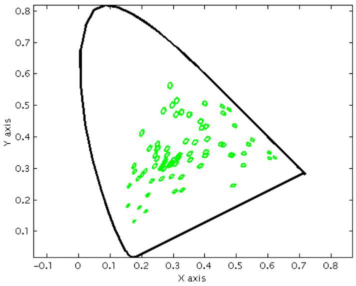

(a) CIELAB ellipses using BFD-P data.

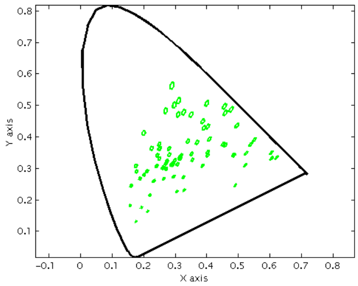

(b) CIELUV ellipses using BFD-P data.

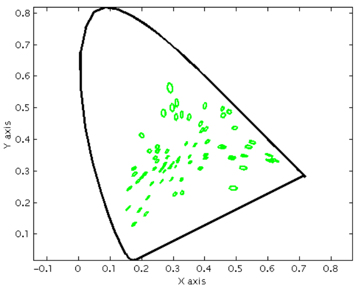

(c) CIEDE00 ellipses using BFD-P data.

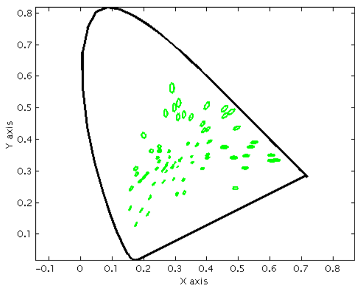

(d) OSA-UCS ΔE_E ellipses using BFD-P data.

Figure 3: Computed CIELAB, CIELUV, Riemannized CIEDE00 and OSA-UCS ΔE_E ellipses in the CIE1964 chromaticity diagram (enlarged 1.5 times).

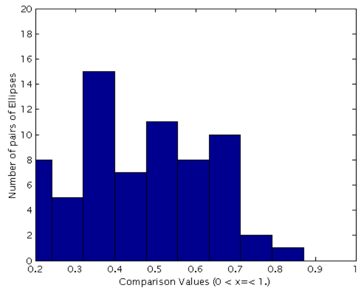

(a) CIELAB.

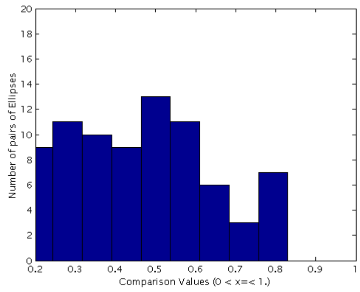

(b) CIELUV.

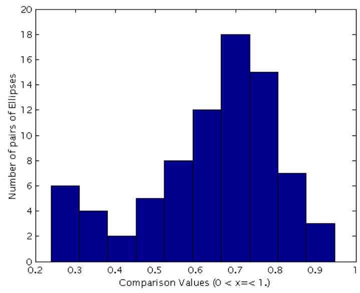

(c) CIEDE00.

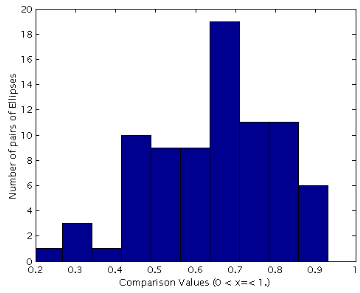

(d) OSA-UCS ΔE_E .

Figure 4: Histogram of comparison values of CIELAB, CIELUV, Rie4annized CIEDE00 and OSA-UCS ΔE_E with respet to BFD-P Ellipses. The values lie in the range $0 < x \leq 1$. Higher comparison value indicates better matching between a pair of ellipses.

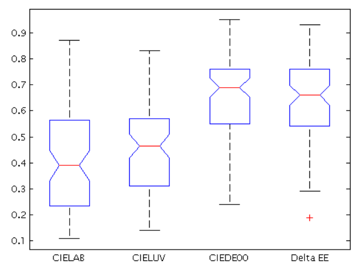

Figure 5: Box plots of ellipse matching values of CIELAB, CIELUV, Riemannized CIEDE00 and OSA-UCS ΔE_E with respect to BFD-P ellipses.

Acknowledgments

The authors would like to give special thanks of gratitude to Dr. Michael Brill for his insightful comments and discussions based upon preliminary results of this research [39]. Similarly, the authors are greatful to the anonymous reviewer for giving us valuable comments and suggestions.

References

[1] R. G. Kuehni, "Threshold color differences compared to super-threshold color differences," Color Res. Appl. **25**, 226–229 (2000).

[2] K. Chickering, "Optimization of the MacAdam modified 1965 friele color-difference formula," J. Optical Society of America **57**, 537 (1967).

[3] CIE, "Recommendations on uniform colour spaces, colour difference equations and psychometric color terms," Tech. Rep. 15, CIE Central Bureau, Vienna (1978).

[4] D. MacAdam, "Visual sensitivities to color differences in daylight," J. Optical Society of America **32**, 247–274 (1942).

[5] W. Brown, "Colour discrimination of twelve observers," J. Optical Society of America **47**, 137–143 (1957).

[6] G. Wyszecki and Fielder, "New color-matching ellipses," J. Optical Society of America **61**, 1135–1152 (1971).

[7] M. R. Luo and B. Rigg, "Chromaticity-discrimination ellipses for surface colours," Color Res. Appl. **11**, 25–42 (1986).

[8] R. Berns, D. H. Alman, L. Reniff, G. Snyder, and M. Balonon-Rosen, "Visual determination of suprathreshold color-difference tolerances using probit analysis," Color Res. Appl. **16**, 297–316 (1991).

[9] K. Witt, "Geometric relations between scales of small colour differences," Color Res. Appl. **24**, 78–92 (1999).

[10] G. Riemann, "Über die Hypothesen, welche der Geometrie zu Grunde liegen," Abh Königl Ges Wiss Göttingen **12**, 133–152 (1868).

[11] H. von Helmholtz, "Das psychophysische Gesetz auf die Farbunterschiede trichromatischer Auge anzuwenden," Psychol. Physiol. Sinnesorgane **3**, 1–20 (1892).

[12] E. Schrödinger, "Grundlinien einer Theorie der Farbenmetrik im Tagessehen," Annalen der Physik **4**, 397–426 (1920).

[13] W. Stiles, "A modified Helmholtz line element in brightness-colour space," in "Proc. Phys. Soc. London," (1946), pp. 41–65.

[14] J. Vos and P. Walraven, "An analytical description of the line element in the zone fluctuation model of color vision," J. Vision Research **12**, 1345–1365 (1972).

[15] J. Vos, “From lower to higher colour metrics: a historical account,” Clinical and Experimental Optometry **89**, 348–360 (2006).

[16] J. Vos and P. Walraven, “Back to Helmholtz,” Color Res. Appl. **16**, 355–359 (1991).

[17] Wyszecki and Stiles, *Color Science: Concepts and Methods, Quantitative Data and Formula* (John Wiley and Sons, New York, 2000), 2nd ed.

[18] M. Luo, G. Cui, and B. Rigg, “The development of the CIE2000 colour difference formula,” Color Res. Appl. **26**, 340–350 (2001).

[19] C. Oleari, M. Melgosa, and R. Huertas, “Euclidean colour difference formula for small-medium colour differences in log-compressed OSA-UCS space,” J. Optical Society of America **26**, 121–134 (2009).

[20] CIE, “Industrial colour difference evaluation,” Tech. Rep. 116, CIE Central Bureau, Vienna (1995).

[21] D. Kim and J. Nobbs, “New weighting functions for the weighted CIELAB colour difference formula,” in “Proceedings of AIC Colour,” (AIC, Kyoto, 1997), pp. 446–449.

[22] CIE, “Improvement to industrial color–difference evaluation,” Tech. Rep. 142, CIE central bureau, Vienna (2001).

[23] J. Gay and R. Hirschler, “Field trials for CIEDE2000: Correlation of visual and instrumental pass/fail decisions in industry.” Tech. Rep. ISBN 390190621, 25th, The CIE Session, San Diego (2003).

[24] M. Melgosa, R. Huertas, and R. S. Berns, “Performance of recent advanced color difference fromulae using the standardized residual sum of squares index,” J. Optical Society of America **25**, pp. 1828–1834 (2008).

[25] P. Urban, M. R. Rosen, and R. S. Berns, “Embedding non-euclidean color spaces into euclidean color spaces with minimal isometric disagreement,” Optical Society of America **27** (2007).

[26] R. G. Kuehni, *Color Space and its Division* (John Wiley and Sons, New York, 2003).

[27] W. Schultze, “The usefulness of colour difference formulas for fixing colour tolerances,” in “AIC Proceedings,” (1972), pp. 254–265.

[28] D. Judd, “Ideal color space: Curvature of color space and its implications for industrial color tolerances,” Palette **29**, 21–28 (1968).

[29] L. Silberstein, “Notes on W.S. Stiles paper entitled : A modified Helmholtz line-element in brightness-colour space,” J. Optical Society of America **37**, pp. 292–295 (1947).

[30] C. Alder, K. P. Chaing, T. F. Chong, E. Coates, A. A. Khalili, and B. Rigg, “Uniform chromaticity scales – new experimental data,” Society of Dyers and Colurist, UK **98**, 14–20 (1982).

[31] D. R. Pant and I. Farup, "Evaluating color difference formulae by Riemannian metric," in "5th European Conference on Colour in Graphics, Imaging, and Vision, CGIV 2010," (Joensuu, Finland, 2010), p. 497.

[32] G. B. Thomas and R. L. Finney, *Calculus and Analytic Geometry* (Addision-Wesley, Massachusetts, 1988).

[33] H. G. Völz, "Euclidization of the first quadrant of the CIEDE2000 color difference system for the calculation of large color differences," Color Res. Appl. **31**, 5–12 (2006).

[34] G. Sharma, W. Wu, and E. N. Dalal, "The CIEDE2000 color-difference formula: Implementation notes, supplementary test data, and mathematical observations," Color Res. Appl. **30**, 21–30 (2004).

[35] C. Oleari, "Color opponencies in the system of the uniform color scales of the Optical Society of America," J. Optical Society of America **21**, 677–682 (2004).

[36] C. Oleari, "Hypotheses for chromatic opponency functions and their performance on classical psychophysical data," Color Res. Appl. **30**, 31–41 (2005).

[37] R. S. Berns, *Principles of Color Technology* (John Wiley and Sons, New York, 2000).

[38] C. Oleari, "Uniform color space for 10 degree visual field and OSA uniform color scales," J. Optical Society of America **10**, pp. 1490–1498 (1993).

[39] D.R.Pant and I. Farup, "Riemannian formulation of the CIEDE2000 color difference formula," in "18th Color and Imaging Conference," (IS&T, 2010), pp. 103–108.

Appendix: Detailed expressions for the Jacobians

From x, y, Y to X, Y, Z

$$\frac{\partial(X,Y,Z)}{\partial(x,y,Y)} = \begin{bmatrix} \frac{\partial X}{\partial x} & \frac{\partial X}{\partial y} & \frac{\partial X}{\partial Y} \\ \frac{\partial Y}{\partial x} & \frac{\partial Y}{\partial y} & \frac{\partial Y}{\partial Y} \\ \frac{\partial Z}{\partial x} & \frac{\partial Z}{\partial y} & \frac{\partial Z}{\partial Y} \end{bmatrix} = \begin{bmatrix} \frac{Y}{y} & \frac{-xY}{y^2} & \frac{x}{y} \\ 0 & 0 & 1 \\ \frac{-Y}{y} & \frac{(x-1)Y}{y^2} & \frac{1-x-y}{y} \end{bmatrix} \tag{59}$$

From X, Y, Z to L^*, a^*, b^*

$$\begin{aligned} \frac{\partial(L,a,b)}{\partial(X,Y,Z)} &= \begin{bmatrix} \frac{\partial L}{\partial X} & \frac{\partial L}{\partial Y} & \frac{\partial L}{\partial Z} \\ \frac{\partial a}{\partial X} & \frac{\partial a}{\partial Y} & \frac{\partial a}{\partial Z} \\ \frac{\partial b}{\partial X} & \frac{\partial b}{\partial Y} & \frac{\partial b}{\partial Z} \end{bmatrix} \\ &= \begin{bmatrix} 0 & \frac{116}{3}(\frac{1}{Y_r})^{\frac{1}{3}} Y^{\frac{-2}{3}} & 0 \\ \frac{500}{3}(\frac{1}{X_r})^{\frac{1}{3}} X^{\frac{-2}{3}} & \frac{-500}{3}(\frac{1}{Y_r})^{\frac{1}{3}} Y^{\frac{-2}{3}} & 0 \\ 0 & \frac{200}{3}(\frac{1}{Y_r})^{\frac{1}{3}} Y^{\frac{-2}{3}} & \frac{-200}{3}(\frac{1}{Z_r})^{\frac{1}{3}} Z^{\frac{-2}{3}} \end{bmatrix} \end{aligned} \tag{60}$$

From X, Y, Z to L^*, u^*, v^*

$$\frac{\partial(L^*,u^*,v^*)}{\partial(X,Y,Z)} = \begin{bmatrix} \frac{\partial L^*}{\partial X} & \frac{\partial L^*}{\partial Y} & \frac{\partial L^*}{\partial Z} \\ \frac{\partial u^*}{\partial X} & \frac{\partial u^*}{\partial Y} & \frac{\partial u^*}{\partial Z} \\ \frac{\partial v^*}{\partial X} & \frac{\partial v^*}{\partial Y} & \frac{\partial v^*}{\partial Z} \end{bmatrix}, \tag{61}$$

where the calculations of all partial derivatives are as follows:

$$\frac{\partial L^*}{\partial X} = 0, \tag{62a}$$

$$\frac{\partial L^*}{\partial Y} = \frac{116}{3}(\frac{1}{Y_r})^{\frac{1}{3}} Y^{(-2/3)}, \tag{62b}$$

$$\frac{\partial L}{\partial Z} = 0, \tag{62c}$$

$$\frac{\partial u^*}{\partial X} = 13\left(116\left(\frac{Y}{Y_r}\right)^{(1/3)} - 16\right)\left[\frac{60Y+12Z}{(X+15Y+3Z)^2}\right], \tag{62d}$$

$$\begin{aligned} \frac{\partial u^*}{\partial Y} &= 13\times\left(116\left(\frac{Y}{Y_r}\right)^{(1/3)} - 16\right)\left[\frac{-60\mathrm{X}}{(X+15Y+3Z)^2}\right] \\ &+ \left[\frac{4X}{(X+15Y+3Z)}\right]\left(\frac{13\times 116(\frac{1}{Y_r})^{\frac{1}{3}} Y^{(-2/3)}}{3}\right) \\ &- \left(\frac{4X_r}{X_r+15Y_r+3Z_r}\right)\left(\frac{13\times 116(\frac{1}{\mathrm{Y_r}})^{\frac{1}{3}} \mathrm{Y}^{(-2/3)}}{3}\right), \end{aligned} \tag{62e}$$

$$\frac{\partial u^*}{\partial Z} = 13\left(116\left(\frac{Y}{Y_r}\right)^{(1/3)} - 16\right)\left[\frac{-12X}{(X+15Y+3Z)^2}\right], \tag{62f}$$

$$\frac{\partial v^*}{\partial X} = 13\left(116\left(\frac{Y}{Y_r}\right)^{(1/3)} - 16\right)\left[\frac{-9\mathrm{Y}}{(X+15Y+3Z)^2}\right], \tag{62g}$$

$$\begin{aligned} \frac{\partial v^*}{\partial Y} &= 13\left(116\left(\frac{Y}{Y_r}\right)^{(1/3)} - 16\right)\left[\frac{9\mathrm{X}+27\mathrm{Z}}{(X+15Y+3Z)^2}\right] \\ &+ \left[\frac{9\mathrm{Y}}{(X+15Y+3Z)}\right]\left(\frac{13\times 116(\frac{1}{Y_r})^{\frac{1}{3}} Y^{(-2/3)}}{3}\right) \\ &- \left(\frac{9Y_r}{X_r+15Y_r+3Z_r}\right)\left(\frac{13\times 116(\frac{1}{\mathrm{Y_r}})^{\frac{1}{3}} \mathrm{Y}^{(-2/3)}}{3}\right), \end{aligned} \tag{62h}$$

$$\frac{\partial v^*}{\partial Z} = 13\left(116\left(\frac{Y}{Y_r}\right)^{(1/3)} - 16\right)\left[\frac{-27\mathrm{Y}}{(X+15Y+3Z)^2}\right]. \tag{62i}$$

From $L^{'}$, $a^{'}$, $b^{'}$ to L', C', h'

The Jacobian for this transformation is

$$\frac{\partial(L',C',h')}{\partial(L^{'},a^{'},b^{'})} = \begin{bmatrix} \frac{\partial L'}{\partial L^{'}} & \frac{\partial L'}{\partial a^{'}} & \frac{\partial L'}{\partial b^{'}} \\ \frac{\partial C'}{\partial L^{'}} & \frac{\partial C'}{\partial a^{'}} & \frac{\partial C'}{\partial b^{'}} \\ \frac{\partial h'}{\partial L^{'}} & \frac{\partial h'}{\partial a^{'}} & \frac{\partial h'}{\partial b^{'}} \end{bmatrix} = \begin{bmatrix} 1 & 0 & 0 \\ 0 & \frac{\partial C'}{\partial a^{'}} & \frac{\partial C'}{\partial b^{'}} \\ 0 & \frac{\partial h'}{\partial a^{'}} & \frac{\partial h'}{\partial b^{'}} \end{bmatrix}. \tag{63}$$

where the partial derivatives are as follows:

$$\frac{\partial C^{'}}{\partial a^{'}} = \frac{a^{'}}{\sqrt{a'^2 + b'^2}} = \frac{a^{'}}{C'} \tag{64a}$$

$$\frac{\partial C^{'}}{\partial b^{'}} = \frac{b^{'}}{\sqrt{a'^2 + b'^2}} = \frac{b'}{C'} \tag{64b}$$

$$\frac{\partial h^{'}}{\partial a^{'}} = \frac{-b'}{C'^2} \tag{64c}$$

$$\frac{\partial h'}{\partial b'} = \frac{a^{'}}{C'^2} \,. \tag{64d}$$

From L^*, a^*, b^* to L', a', b'

The Jacobian for this transformation is

$$\frac{\partial(L', a', b')}{\partial(L^*, a^*, b^*)} = \begin{bmatrix} \frac{\partial L'}{\partial L^*} & \frac{\partial L'}{\partial a^*} & \frac{\partial L'}{\partial b^*} \\ \frac{\partial a'}{\partial L^*} & \frac{\partial a'}{\partial a^*} & \frac{\partial a'}{\partial b^*} \\ \frac{\partial b'}{\partial L^*} & \frac{\partial b'}{\partial a^*} & \frac{\partial b'}{\partial b^*} \end{bmatrix} = \begin{bmatrix} 1 & 0 & 0 \\ 0 & \frac{\partial a'}{\partial a^*} & \frac{\partial a'}{\partial b^*} \\ 0 & \frac{\partial b'}{\partial a^*} & \frac{\partial b'}{\partial b^*} \end{bmatrix} . \tag{65}$$

$$\frac{\partial a^{'}}{\partial a^*} = \left[(1+G) + \frac{a^{*2}}{C^*} \left(-\frac{1}{4} \frac{7 \times 25^7 C^{*5/2}}{(C^{*7} + 25^7)^{3/2}} \right) \right] , \tag{66a}$$

$$\frac{\partial a^{'}}{\partial b^*} = \frac{a^* b^*}{C^*} \left(-\frac{1}{4} \frac{7 \times 25^7 C^{*5/2}}{(C^{*7} + 25^7)^{3/2}} \right) , \tag{66b}$$

$$\frac{\partial b^{'}}{\partial a^*} = 0 \tag{66c}$$

$$\frac{\partial b'}{\partial b^*} = 1 \,. \tag{66d}$$

From L_{OSA}, G, J to L_E, G_E, J_E

$$\frac{\partial(L_E, G_E, J_E)}{\partial(L_{OSA}, G, J)} = \begin{bmatrix} \frac{\partial L_E}{\partial L_{OSA}} & \frac{\partial L_E}{\partial G} & \frac{\partial L_E}{\partial J} \\ \frac{\partial G_E}{\partial L_{OSA}} & \frac{\partial G_E}{\partial G} & \frac{\partial G_E}{\partial J} \\ \frac{\partial J_E}{\partial L_{OSA}} & \frac{\partial J_E}{\partial G} & \frac{\partial J_E}{\partial J} \end{bmatrix} , \tag{67}$$

where the calculation of all partial derivatives are as follows:

$$\frac{\partial L_E}{\partial L_{OSA}} = \frac{10}{a_L + 10b_L L_{OSA}}, \tag{68a}$$

$$\frac{\partial L_E}{\partial G} = 0, \tag{68b}$$

$$\frac{\partial L_E}{\partial J} = 0, \tag{68c}$$

$$\frac{\partial G_E}{\partial L_{OSA}} = 0, \tag{68d}$$

$$\frac{\partial G_E}{\partial G} = -\left(\frac{C_E}{C_{OSA}} + G\left[\frac{C_{OSA}(10/a_c + 10b_c C_{OSA}) - C_E}{C_{OSA}^2}\right]\frac{G}{C_{OSA}}\right), \tag{68e}$$

$$\frac{\partial G_E}{\partial J} = -G\left[\frac{C_{OSA}(10/a_c + 10b_c C_{OSA}) - C_E}{C_{OSA}^2}\right]\frac{J}{C_{OSA}}, \tag{68f}$$

$$\frac{\partial J_E}{\partial L_{OSA}} = 0, \tag{68g}$$

$$\frac{\partial J_E}{\partial G} = -J\left[\frac{C_{OSA}(10/a_c + 10b_c C_{OSA}) - C_E}{C_{OSA}^2}\right]\frac{G}{C_{OSA}}, \tag{68h}$$

$$\frac{\partial J_E}{\partial J} = -\left(\frac{C_E}{C_{OSA}} + J\left[\frac{C_{OSA}(10/a_c + 10b_c C_{OSA}) - C_E}{C_{OSA}^2}\right]\frac{J}{C_{OSA}}\right). \tag{68i}$$

From x, y, Y to L_{OSA}

$$\frac{\partial L_{OSA}}{\partial(x,y,Y)} = \frac{\partial L_{OSA}}{\partial Y_0}\begin{bmatrix}\frac{\partial Y_0}{\partial x} & \frac{\partial Y_0}{\partial y} & \frac{\partial Y_0}{\partial Y}\end{bmatrix}, \tag{69}$$

where

$$\frac{\partial L_{OSA}}{\partial Y_0} = 5.9\left[\frac{1}{3}Y_0^{-2/3} + 0.042 \cdot \frac{1}{3}(Y_0 - 30)^{-2/3}\right]\frac{1}{\sqrt{2}}, \tag{70a}$$

$$\frac{\partial Y_0}{\partial x} = Y(4.4934 \cdot 2x - 4.2760y - 1.3744), \tag{70b}$$

$$\frac{\partial Y_0}{\partial y} = Y(4.3034 \cdot 2y - 4.2760x - 2.5643), \tag{70c}$$

$$\frac{\partial Y_0}{\partial Y} = 4.4934x^2 + 4.3034y^2 - 4.2760xy - 1.3744x - 2.5643y + 1.8103. \tag{70d}$$

From L_{OSA}, A, B, C to G, J

$$\frac{\partial(G,J)}{\partial(L_{OSA},A,B,C)} = \begin{bmatrix}\frac{\partial G}{\partial L_{OSA}} & \frac{\partial G}{\partial A} & \frac{\partial G}{\partial B} & \frac{\partial G}{\partial C} \\ \frac{\partial J}{\partial L_{OSA}} & \frac{\partial J}{\partial A} & \frac{\partial J}{\partial B} & \frac{\partial J}{\partial C}\end{bmatrix}, \tag{71}$$

where

$$\frac{\partial G}{\partial L_{OSA}} = T_G \frac{\partial S_G}{\partial L_{OSA}} = T_G \cdot -2 \times 0.764, \tag{72a}$$

$$\frac{\partial J}{\partial L_{OSA}} = T_J \frac{\partial S_J}{\partial L_{OSA}} = T_J \cdot 2 \times 0.57354, \tag{72b}$$

$$\frac{\partial G}{\partial A} = S_G \frac{0.9482}{A}, \tag{72c}$$

$$\frac{\partial G}{\partial B} = S_G \frac{-0.9482 - 0.3175}{B}, \tag{72d}$$

$$\frac{\partial G}{\partial C} = S_G \frac{0.3175}{C}, \tag{72e}$$

$$\frac{\partial J}{\partial A} = S_J \frac{0.1792}{A}, \tag{72f}$$

$$\frac{\partial J}{\partial B} = S_J \frac{-0.1792 + 0.9837}{B}, \tag{72g}$$

$$\frac{\partial J}{\partial C} = S_J \frac{-0.9837}{C}, \tag{72h}$$

where the shorthands

$$T_G = 0.9482[\ln A - \ln(0.9366B)] - 0.3175[\ln B - \ln(0.9807C)], \tag{73a}$$

$$T_J = 0.1792[\ln A - \ln(0.9366B)] + 0.9837[\ln B - \ln(0.9807C)], \tag{73b}$$

have been introduced.